



HAL
open science

Rotation of millimeter-size objects using ordinary light

Olivier Emile, Janine Emile

► **To cite this version:**

Olivier Emile, Janine Emile. Rotation of millimeter-size objects using ordinary light. *Optics Letters*, 2016, 41 (2), pp.211-214. 10.1364/OL.41.000211 . hal-01248554

HAL Id: hal-01248554

<https://hal.science/hal-01248554>

Submitted on 28 Dec 2015

HAL is a multi-disciplinary open access archive for the deposit and dissemination of scientific research documents, whether they are published or not. The documents may come from teaching and research institutions in France or abroad, or from public or private research centers.

L'archive ouverte pluridisciplinaire **HAL**, est destinée au dépôt et à la diffusion de documents scientifiques de niveau recherche, publiés ou non, émanant des établissements d'enseignement et de recherche français ou étrangers, des laboratoires publics ou privés.

Rotation of millimeter-size objects using ordinary light.

Olivier Emile¹ and Janine Emile²

¹*Université de Rennes 1, 35042 Rennes Cedex, France.**

²*IPR, UMR 6251, CNRS, Université de Rennes 1, 35042 Rennes Cedex, France.*

(Dated: December 30, 2015)

Abstract

The ability to optically rotate bodies offers new degrees of control of micro-objects with applications in various domains including micro-electromechanical-systems (MEMS), biomanipulations or optofluidics. Here we demonstrate the optically induced rotation of simple asymmetric two-dimensional objects using plane waves originating either from ordinary laser sources or from black body radiation. The objects are floating on an air/water interface. We observe a steady state rotation depending on the light intensity and on the asymmetry of the object. We interpret this rotation in terms of light diffraction by the edges of the object. Such systems could be easily implemented in optofluidic devices to induce liquid flow without the need for special light sources.

OCIS Codes (050.4865) Optical vortices; (350.4855) Optical tweezers or optical manipulation; (260.3160) Interference

Since 1992, there has been a renew of interest for the angular momentum of light [1, 2]. Besides from fundamental considerations, there are many potential applications as, for example, in astrophysics [3], in optical tweezers for biological manipulations [2, 4–6], in telecommunications [7–9], or in quantum optics [10–14]. The light beams are generally produced either from dedicated optical elements such as dove prisms and lenses or from the diffraction of particular gratings [1, 15]. We have recently shown experimentally that such beams could also be produced by the diffraction of plane waves from two-dimensional asymmetric objects [16]. We have then conjectured that, due to the law of angular momentum conservation, the diffracting object must acquire angular momentum and start to rotate.

The rotation of small objects by light sources has many applications in various domains including MEMS [2, 17], biomanipulation [5, 6] or optofluidics [18, 19]. Up to now, two major schemes have successfully enabled such rotations, based either on the linear momentum or on the angular momentum of light. The first scheme takes advantages of specially shaped three-dimensional objects and the scattering of ordinary light [20–22], whereas, the latter, relies either on the spin [23–26] or on the Orbital Angular Momentum (OAM) [27–29] of light from dedicated sources, coupled with the absorbing or birefringent optical properties of the object. One may then wonder whether it could be possible to rotate ordinary objects with ordinary light. The aim of the letter is thus to investigate the rotational properties of asymmetrical objects floating in a water tank and lighted up by ordinary sources. The experimental set-up is sketched on figure 1. The rotating objects are 1.5-mm radius two-dimensional paddle wheels printed on 2-mm radius symmetric disks cut out an ordinary laser printer transparency. They could also be called cams or ratchet wheels. The printed paddle wheels have up to eight blades. The printed surfaces of the paddle wheels are constant whatever the number of blades on our printings. The disks, are floating on a tank filled with ordinary water at a temperature of 20°C. The water enables the disks to rotate around their own axis

in the plane of the air/water interface.

Since the disks are symmetrical, the rotation cannot be attributed to the Brownian motion observed for self-propelling asymmetrical particles [30]. Besides, we are neither interested in the surface deformation [31] by capillary interactions nor in the frictional resistance of the fluid surrounding the object that can be found with asymmetric objects [32]. Moreover, this shape minimizes the friction between the object and the water flow around it. The light comes out an optical fiber connected either to a 980 nm-laser diode (IDIL) or a cold light source (Schott 1500 LCD) generating black body radiation. The fiber is fixed to a mechanical support that can be translated in the plane of the table in order to track the paddle wheel. The rotation is detected with a camera that is also sensitive to the 980 nm radiation.

Figure 2 shows the rotation of a three blades paddle wheel ($p = 3$), for different times of laser exposure and for a light power of 80 mW at the end of the fiber. The rotation speed is clockwise and is of the order of $0.1^\circ/\text{s}$. Because the transient regime is in the microsecond range, like for submillimeter-sized objects in liquid or at air/liquid interface [20–24, 27], the steady-state rotation is easily observed by a standard camera. Contrarily, for centimeter size objects suspended in air [33], the accelerating regime is mainly evidenced. Then the fluid, the size of the object and the experimental environment influence the rotational dynamics. The optical fiber is set so that the light impinges perpendicular to the air/water interface and illuminates the paddle wheel uniformly.

According to previous calculations [16], the diffracted light in the shadow of the paddle wheel carries orbital angular momentum with a topological charge ℓ that is proportional to the number of blades p . Moreover, in this case, the phase of the diffracted beam, in a plane parallel to the interface, rotates counter clockwise. Due to the law of angular momentum conservation, a torque (mechanical angular momentum) on the paddle wheel must counterbalance this light orbital an-

gular momentum generation. The disk should then rotate clockwise, as observed. More generally, every asymmetrical plane object should rotate. For example, we found experimentally that besides for various paddle wheels, a drawing mimicking a lemna minor shape, a maple seed, an insect's egg, or any two-dimensional asymmetrical object indeed rotates (see figure 1). Such objects can also be obtained by aggregation of nanoparticles in dipalmitoylphosphatidylcholine monolayers [34] modeling lung surfactant monolayers.

Following the preceding argument, a reverse paddle wheel should rotate the other way around. Let us thus reverse the object floating on the water. The diffracted beam then carries angular momentum with opposite topological charges. Its phase rotates clockwise. Thus the object rotates counter clockwise as can be noticed on figure 3. Note that a two-dimensional object like a printed paddle wheel cannot be chiral. However, when this object is floating on an interface between two media with different optical indices, one can always draw the normal to the interface. This floating asymmetric plane object becomes thus chiral when taking into account the interface.

Because the topological charge of the diffracted beam is proportional to the number of blades on the wheel [16], one would then expect the rotation speed to increase with this number, for a given constant surface of the paddle wheel printed on the disk. This is experimentally evidenced, in figure 3. We have plotted the rotation speed versus time for different paddle wheels up to $p = 6$. One clearly sees that the rotation speed increases with p . However, the variation seems not to be linear, especially for high p values.

Figure 4 shows the experimental rotation speed versus the number of blades up to $p = 8$. The rotation speed saturates and even decreases, having a maximum value around $p = 6$. We have also calculated numerically the electric field $\vec{E}(\vec{r})$ at a distance D from the mask and at a distance r from the axis, using Fresnel

diffraction

$$\vec{E}(\vec{r}) \propto \iint \frac{e^{i\vec{k}(\vec{r}-\vec{r}')}T(\vec{r}')}{\sqrt{D^2 + |\vec{r}-\vec{r}'|^2}}\vec{E}(\vec{r}')r'dr'd\theta' \quad (1)$$

where $\vec{E}(\vec{r}')$ is the radial dependence of the incident beam amplitude impinging on the mask and $T(\vec{r}')$ is the mask transmission. Typically, $T(\vec{r}') = 0$ on the mask and $T(\vec{r}') = 1$ otherwise. \vec{k} is the wave vector. Assuming a Gaussian distribution of the amplitude of the incident field one can write

$$\vec{E}(\vec{r}', \theta) = E_0 e^{-\frac{r'^2}{w^2}} \vec{e}_0 \quad (2)$$

where w is the beam waist and \vec{e}_0 is the light polarization. One can note that since the mask is invariant under a $2\pi/p$ rotation, the field at a distance D has the same invariance, i.e.

$$\vec{E}(r, \theta + 2\pi/p) = \vec{E}(r, \theta) \quad (3)$$

where θ is the azimuthal angle.

From equation 1, we have numerically extracted the OAM of the field and the torque. Then, considering E_0 as the only adjusting parameter for all the paddle wheels, we have plotted on figure 4, the rotation speed versus the number of blades. The experimental values and the calculated ones superimposed exactly, confirming the saturation effect. This saturation could be attributed to the fact that the intensity of the diffracted beam decreases when increasing p , for a given surface of the paddle wheel. The ratchet character of the paddle wheel is then less pronounced when increasing p . One could not totally exclude a damping by the water and a transfer of angular momentum to the fluid. However, here, the diffracting figure is printed on a symmetric disk floating on the water that minimizes the interaction with the water flow. It is thus more likely that this saturation is due to the decrease of asymmetry of the diffracting picture when increasing p .

From equation 1, the diffracted amplitude is proportional to E_0 , the incoming amplitude, as always for diffraction effects. Then the torque must be proportional

to the light intensity. We find experimentally a linear variation of the rotation speed with the laser power, as could be expected. We have checked with a polarizer, that the light impinging on the object is linearly polarized, with a fixed direction. Then, the rotational effect cannot be attributed to the spin angular momentum of light, nor to a rotation of the linear polarization [23, 24]. It could not be due to thermocapillary propulsion observed for asymmetric microgears neither [35] since the paddle wheel we used is printed on a disk which symmetry excludes such effects.

The transfer mechanism is very different from what have been reported up to know in the literature (see for example [2] for a review). It is not due to spin angular momentum transfer neither to OAM, nor to alignment as for birefringent objects. Since the object is a two dimensional object, the rotation could not be induced via linear angular momentum transfer. There is no need for special polarization nor particular phase varying fields nor dedicated objects. Indeed the transfer mechanism is due to the diffraction of a simple and ordinary plane wave by the edges of the printed picture. It could be performed with every asymmetric picture. Note that this transfer mechanism can also rotate symmetric objects. For example, in our case, the object is symmetric and transparent. The diffraction from the edges of a asymmetric printed structure on a transparency makes the whole object to rotate.

Could the effect be also observed with natural light, like for an asymmetrical object, such as bacteria, colloidal particles or macromolecules, under sunlight exposure? We have replaced the laser diode source by the blackbody radiation from a cold lamp used in a microscope system. We have plotted in figure 5, the rotation speed for a three blades ($p = 3$) paddle wheel versus the temperature of the blackbody. We have also measured the radiation power at the end of the fiber. We found that it varies linearly with the temperature within our temperature range. The rotation speed is linear versus the optical power as for the laser diode, despite

some water flows in the tank. They are probably due to temperature gradients (typically 5 K/cm) caused by the absorption of part of the radiation power by the water.

The driven rotation of this paddle wheel can thus even be performed with ordinary light. The induced torque is applied perpendicular to the object, on the object axis like with mechanical motors, but without any contacts. The rotation we report is performed with an asymmetric diffracting paddle wheel. It could be implemented on any support that could be symmetric or not. Besides, there is no restriction concerning the number of blades. For example, we have performed rotation of a $p = 1$ paddle wheel which more looks like a cam or a bacteria (see fig.4). Moreover, although in our case the object is floating at an air/water interface, the experiment could be performed with an underwater object since the transfer mechanism is only governed by diffraction.

The rotation frequency we report here seems very low, of the order of 5.10^{-4} Hz, compared with the rotation rates of micro-objects [23, 24, 27, 35] which are of the order of few hertz. However, let us scale our experiment to $1\mu\text{m}$ diameter objects. Assuming a drag coefficient proportional to the diameter (4 mm here), and focalizing the light from few centimeters (here) to few microns, one would gain a 4.10^3 factor on the drag coefficient and nearly a factor of 6 on the light efficiency transfer. One would find a 12 Hz rotation frequency for a 80 mW laser. Such rotations could find applications in optofluidic devices to optically drive micromotors that would generate liquid flows without the need for special absorbing, reflecting or birefringence properties of the micromotor.

Finally, this rotation of asymmetrical two-dimensional objects floating on an air/liquid interface may shine some new light in the unsettling problem of the homochirality of life [36–38]. Dealing actually with the reverse problem, let us consider the sunlight, and rotating macromolecules or colloidal particles on an air/liquid interface. One could not totally exclude that the combination of light

and rotation may induced some asymmetry on initially symmetrical objects that then leads to chirality.

ACKNOWLEDGMENTS

Acknowledgments. The authors thank Jean René Thébault for technical assistance.

* Corresponding author; olivier.emile@univ-rennes1.fr

- [1] L. Allen, M.W. Beijersbergen, R.J.C. Spreeuw, and J.P. Woerdman, "Orbital angular momentum of light and the transformation of Laguerre-Gaussian laser modes." *Phys. Rev. A* **45**, 8185-8189 (1992).
- [2] M. Padgett and R. Bowman, "Tweezers with a twist." *Nat. Photonics* **5**, 343-348 (2011).
- [3] F. Tamburini, B. Thidé, G. Molina-Terriza, and G. Anzolin, "Twisting of light around rotating black holes." *Nat. Phys.* **7**, 195-197 (2011).
- [4] D.G. Grier, "A revolution in optical manipulation." *Nature* **424**, 810-816 (2003).
- [5] G. Carmon and M. Feingold, "Rotation of single bacterial cells relative to the optical axis using optical tweezers." *Opt. Lett.* **36**, 40-42 (2011).
- [6] J. Lipfert, M.M. van Oene, M. Lee, F. Pedaci, and N.H. Dekker, "Torque spectroscopy for the study of rotary motion in biological systems." *Chem. Rev.* **115**, 1449-1474 (2015).
- [7] I.M. Fazal, N. Ahmed, J. Wang, J.-Y. Yang, Y. Yan, B. Shamee, H. Huang, Y. Yue, S. Dolinar, M. Tur, and A.E. Willner, "2 Tbit/s free-space data transmission on two orthogonal orbital-angular-momentum beams each carrying 25 WDM channels" *Opt. Lett.* **37**, 4753-4755 (2012).
- [8] N. Bozinovic, Y. Yue, Y. Ren, M. Tur, P. Kristensen, H. Huang, A.E. Willner, and S. Ramachandran, "Terabit-scale orbital angular momentum mode division multiplexing in fibers." *Science* **340**, 1545-1548 (2013).
- [9] H. Zhou, J. Dong, L. Shi, D. Huang, and X. Zhang, "Hybrid coding method of multiple orbital angular momentum states based on the inherent orthogonality." *Opt. Lett.* **39**, 731-734 (2015).

- [10] A. Vaziri, G. Weihs, and A. Zeilinger, "Experimental two-photon, three-dimensional entanglement for quantum communication." *Phys. Rev. Lett.* **89**, 240401 (2002).
- [11] J. Leach, B. Jack, J. Romero, A.K. Jha, A.M. Yao, S. Franke-Arnold, D.G. Ireland, R.W. Boyd, S.M. Barnett, and M.J. Padgett, "Quantum correlations in optical angle-orbital angular momentum variables." *Science* **329**, 662-665 (2010).
- [12] V. D'Ambrosio, E. Nagali, C.H. Monken, S. Slussarenko, L. Marrucci, and F. Sciarrino, "Deterministic qubit transfer between orbital and spin angular momentum of single photons." *Opt. Lett.* **37**, 172-174 (2012).
- [13] R. Fickler, R. Lapkiewicz, W.N. Plick, M. Krenn, C. Schaeff, S. Ramelow, and A. Zeilinger, "Quantum entanglement of high angular momenta." *Science* **338**, 640-643 (2012).
- [14] A.J.F de Almeida, S. Barreiro, W.S. Martins, R.A. de Oliveira, D. Felintoi, L. Pruvost, and J.M.R. Tabosa, "Storage of orbital angular momenta of light via coherent population oscillation." *Opt. Lett.* **40**, 2545-2548 (2015).
- [15] A.M. Yao and M.J. Padgett, "Orbital angular momentum: origins, behavior and applications." *Adv. Opt. Photon.* **3**, 161-204 (2011).
- [16] O. Emile, M. le Meur, and J. Emile, "Light angular momentum of a plane wave diffracted by a two-dimensional object." *Phys. Rev. A* **89**, 013846 (2014).
- [17] M.G. Donato, J. Hernandez, A. Mazzulla, C. Provenzano, R. Saija, R. Sayed, S. Vasi, A. Magazzù, P. Pagliusi, R. Bartolino, P.G. Gucciardi, O.M. Maragò, and G. Cipparrone, "Polarization-dependent optomechanics mediated by chiral microresonators." *Nat. Commun.* **5**, 3656 (2014).
- [18] S.L. Neale, M.P. MacDonald, K. Dholakia, and T.F. Krauss, "All-optical control of microfluidic components using form birefringence." *Nat. Mater.* **4**, 530-533 (2005).
- [19] S. Mohanty, "Optically-actuated translational and rotational motion at the microscale for microfluidic manipulation and characterization." *Lab Chip* **12**, 3624-3636 (2012).

- [20] P. Galajda and P. Ormos, "Rotors produced and driven in laser tweezers with reversed direction of rotation." *Appl. Phys. Lett.* **80**, 4653-4655 (2002).
- [21] T.A. Nieminen, S.J.W. Parkin, N.R. Heckenberg, and H. Rubinsztein-Dunlop, "Optical torque and symmetry." *Proc. SPIE* **5514**, 254-263 (2004).
- [22] H. Rubinsztein-Dunlop, T. Asavei, A.B. Stilgoe, V.L.Y. Loke, R. Vogel, T.A. Nieminen, and N.R. Heckenberg, "Design of optically driven microrotors," in *Optical Nano and Micro Actuator Technology*, G. K. Knopf and Y. Otani, eds. (CRC Press, 2012), pp. 277-306.
- [23] M.E.J. Friese, T.A. Nieminen, N.R. Heckenberg, and H. Rubinsztein-Dunlop, "Optical alignment and spinning of laser-trapped microscopic particles." *Nature* **394**, 348-350 (1998).
- [24] L. Paterson, M.P. MacDonald, J. Arlt, W. Sibbett, P.E. Bryant, and K. Dholakia, "Controlled rotation of optically trapped microscopic particles." *Science* **292**, 912-914 (2001).
- [25] A. La Porta and M.D. Wang, "Optical torque wrench: angular trapping, rotation, and torque detection of quartz microparticles." *Phys. Rev. Lett.* **92**, 190801 (2004).
- [26] D.B. Ruffner and D.G. Grier, "Optical conveyors: a class of active tractor beams." *Phys. Rev. Lett.* **108**, 173602 (2012).
- [27] H. He, M.E.J. Friese, N.R. Heckenberg, and H. Rubinsztein-Dunlop, "Direct observation of transfer of angular momentum to absorptive particles from a laser beam with a phase singularity." *Phys. Rev. Lett.* **75**, 826-829 (1995).
- [28] V. Garcés-Chávez, D. McGloin, M.J. Padgett, W. Dultz, H. Schmitzer, and K. Dholakia, "Observation of the transfer of the local angular momentum density of a multiringed light beam to an optically trapped particle." *Phys. Rev. Lett.* **91**, 093602 (2003).
- [29] J. Zhao, I.D. Chremmos, D. Song, D.N. Christodoulides, N.K. Efremidis, and Z. Chen, "Curved singular beams for three-dimensional particle manipulation."

- Sci. Rep. **5**, 12086 (2015).
- [30] F. Kümmel, B. ten Hagen, R. Wittkowski, I. Buttinoni, R. Eichhorn, G. Volpe, H. Löwen, and C. Bechinger, "Circular motion of asymmetric self-propelling particles." *Phys. Rev. Lett.* **110**, 198302 (2013).
- [31] L. Botto, E.P. Lewandowski, M. Cavallaro Jr., and K.J. Stebe, "Capillary interactions between anisotropic particles." *Soft Matter* **8**, 9957-9971 (2012).
- [32] S. Michelin, T.D. Montenegro-Johnson, G. De Canio, N. Lobato-Dauzier, and E. Lauga, "Geometric pumping in autophoretic channels." *Soft Matter* **11**, 5804-5811 (2015).
- [33] O. Emile, C. Brousseau, J. Emile, R. Niemiec, K. Mahdjoubi, and B. Thidé, "Electromagnetically induced torque on a large ring in the microwave range." *Phys. Rev. Lett.* **112**, 053902 (2014).
- [34] K.H. Kim, S.Q. Choi, Z.A. Zell, T.M. Squires, and J.A. Zasadzinski, "Effect of cholesterol nanodomains on monolayer morphology and dynamics." *PNAS* **110**, 3677-3682 (2013).
- [35] C. Maggi, F. Saglimbeni, M. Dipalo, F. De Angelis, and R. Di Leonard, "Micromotors with asymmetric shape that efficiently convert light into work by thermocapillary effects" *Nat. Commun.* **6**, 7855 (2015).
- [36] S.F. Mason, "Origins of biomolecular handedness." *Nature* **311**, 19-23 (1984).
- [37] Y. Tang and A.E. Cohen, "Enhanced enantioselectivity in excitation of chiral molecules by superchiral light." *Science* **332**, 333-336 (2011).
- [38] C. Rosales-Guzmán, K. Volke-Sepulveda, and J.P. Torres, "Light with enhanced optical chirality." *Opt. Lett.* **37**, 3486-3488 (2012).

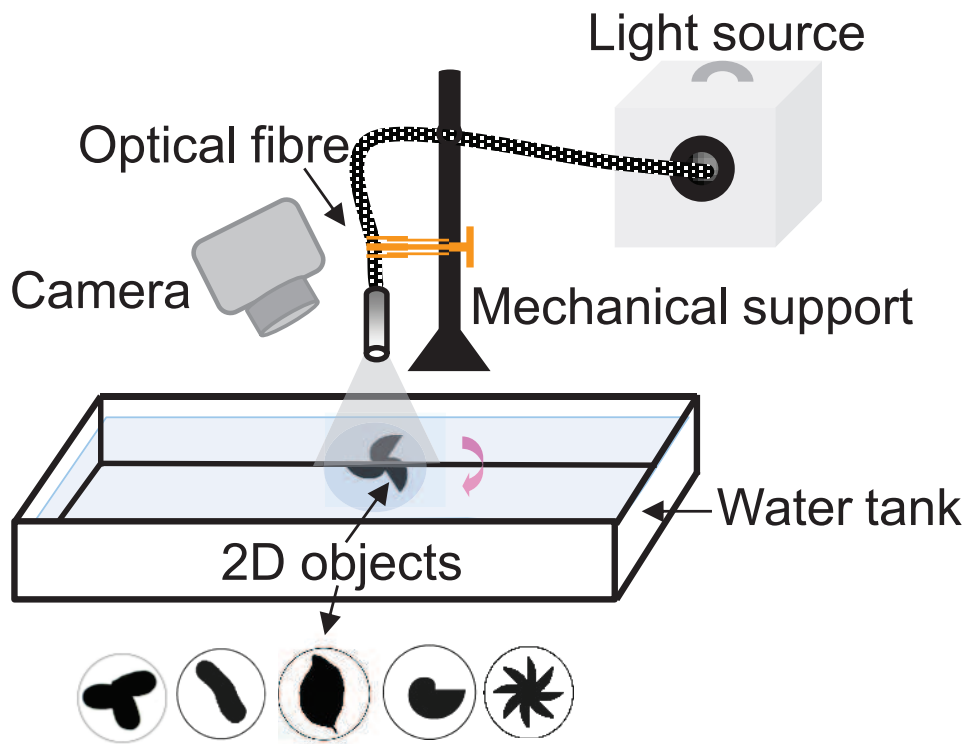


FIG. 1. Experimental set up. Various two-dimensional asymmetrical objects (lemna minor: free floating plant, bacteria, Daphnia: genus of small planktonic crustacean, paddle wheels with $p = 1$ and -8), floating on a tank full of water, start to rotate under the influence of ordinary light coming out of an optical fiber.

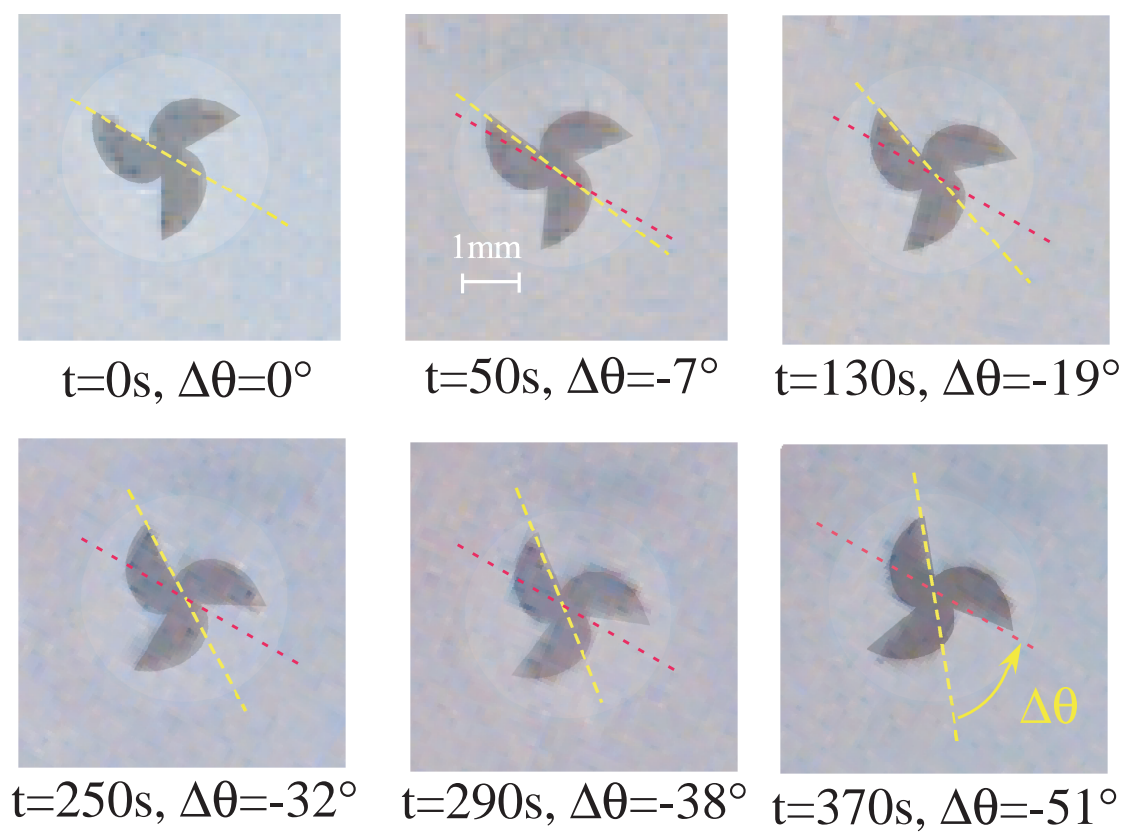


FIG. 2. Rotation of a paddle wheel with three blades versus time. The position of the asymmetrical printed object is recorded for six different times. The yellow dotted line indicates one of the axes of the object. The red dotted line indicates the initial orientation of this axis.

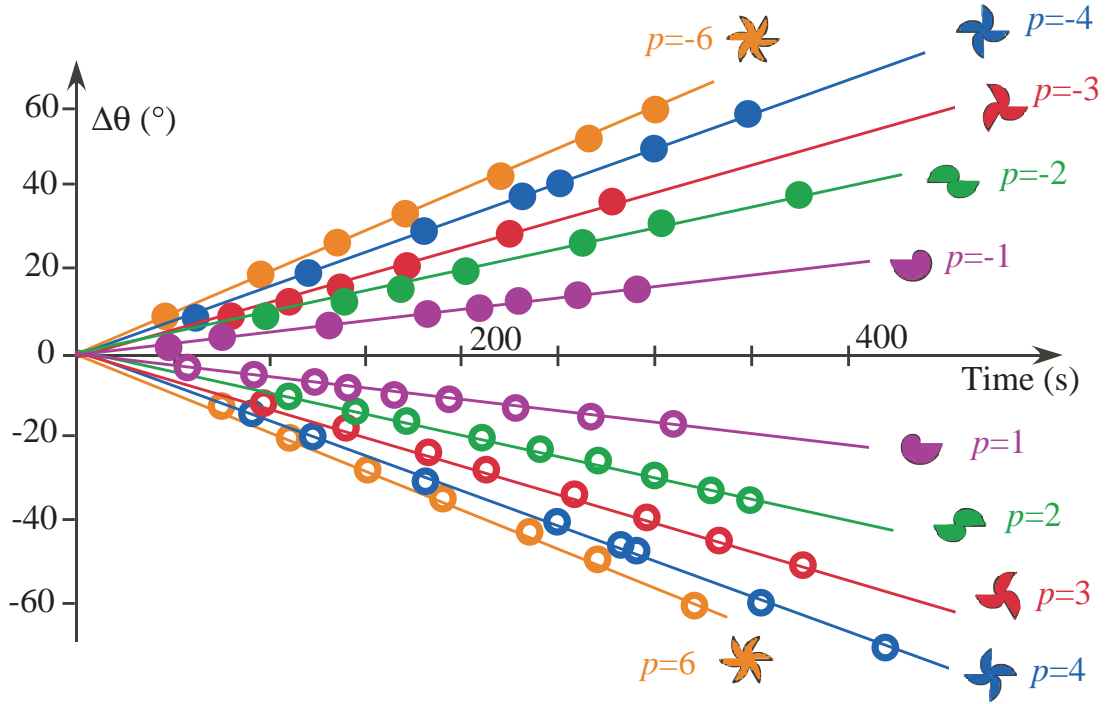


FIG. 3. Rotation of various paddle wheels versus time. Rotation of paddle wheels with p paddles with positive ($p \geq 0$) and negative ($p \leq 0$) orientations. The curves for positive and negative paddle wheels are exactly symmetric. The rotation speed increases with the number of paddles. The error bars are within the points. Note that the paddle wheels have all the same surface.

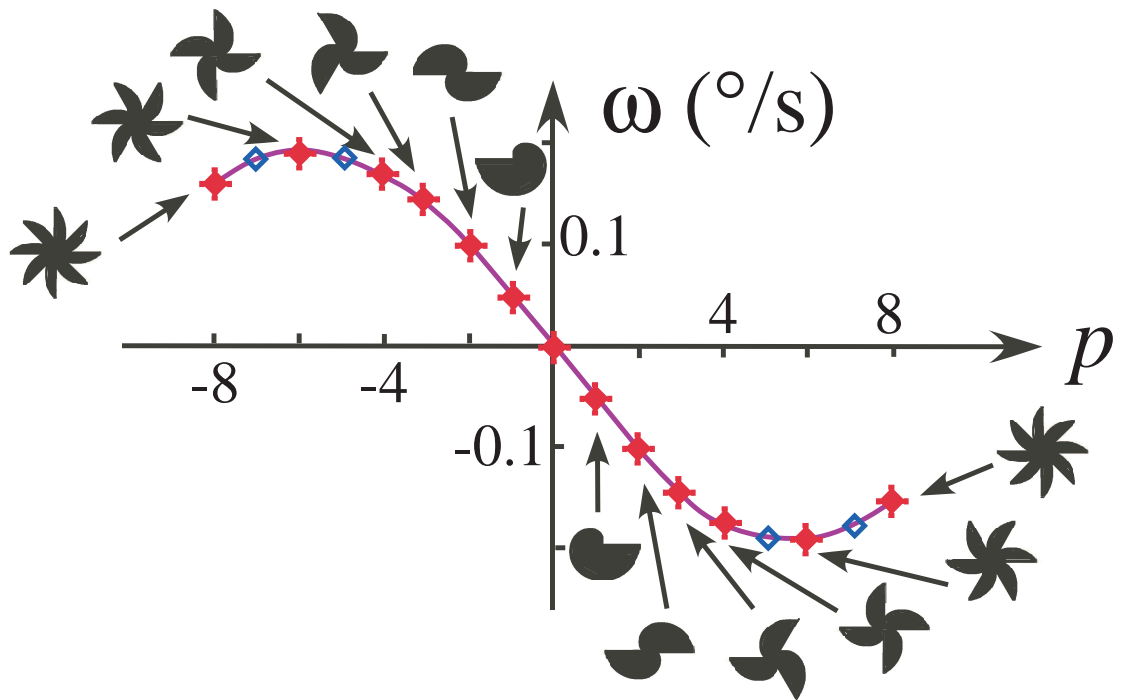


FIG. 4. Angular speed of rotation of paddles. a) Rotation speed versus number of blades. Circle experimental values, open diamonds calculated values. Since the experimental and numerical points exactly superimposed, the diamonds are only visible for $p = 5$ and $p = 7$. The solid line is a guide for the eye.

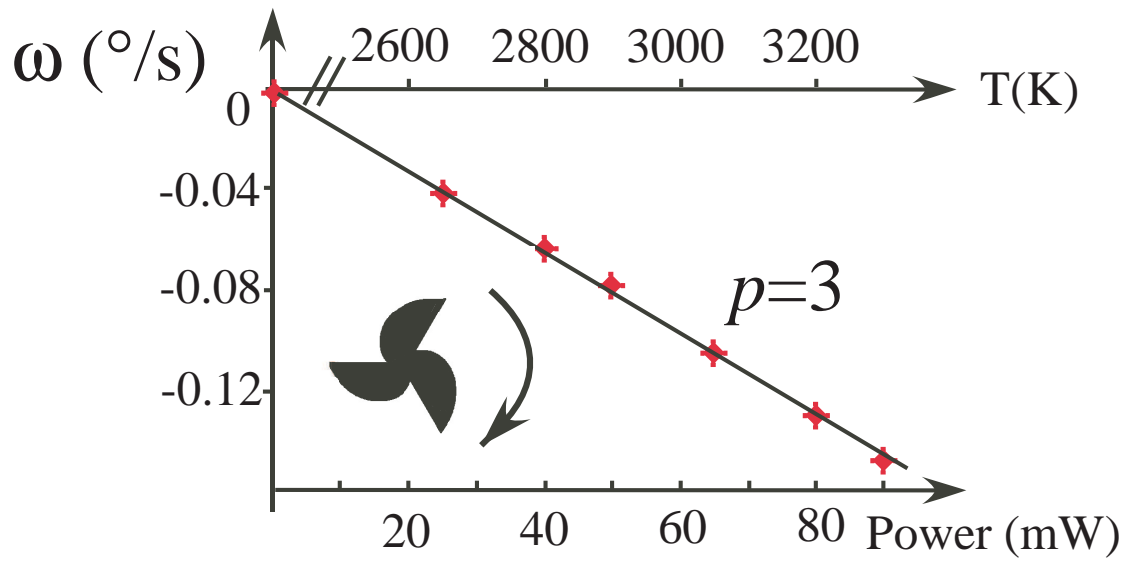


FIG. 5. Linear variation of the rotation speed of the $p = 3$ paddle wheel versus temperature (top) and versus optical power (bottom). The error bars are within the points.